

Supplementary Tables and Figures:

Table S1. Patient demographics in lung cancer observational study

	Age/ Sex	Ethnicity	Diagnosis	Stage	Metastatic disease?	Metastatic site(s)	Prior chemo	Prior rad	Agent 1	Agent 2	Agent 3/4	ICI
USO-004	63/M	Caucasian	NSCLC	IV	Yes	Liver, Mediastinal Nodes	Yes	No	Paclitaxel	Carboplatin		Nivolumab
USO-007	64/F	Caucasian	NSCLC	IV	Yes	Opposite Lung	No	No				Pembrolizum ab
USO-008	73/M	Caucasian	NSCLC	IV	Yes	Opposite Lung	No	No				Pembrolizum ab
USO-010	70/M	Caucasian	NSCLC	IV	Yes	Brain	Yes	No	Carboplatin	Etoposide		Nivolumab + Ipilimumab
USO-013	58/M	African American	NSCLC	IV	Yes	Thyroid, Aortic Nodes, Spleen, Lymph node	Yes	Yes	Vinorelbine	Cisplatin	Carboplatin, Paclitaxel	Nivolumab
USO-027	69/M	Caucasian	NSCLC	IV	Yes	Lymph node	Yes	No	Cisplatin	Etoposide		Nivolumab + Ipilimumab
USO-028	54/M	Caucasian	SCLC	IV	Yes	Liver	Yes	No	Carboplatin	Etoposide		Nivolumab + Ipilimumab
USO-031	92/M	Caucasian	NSCLC	IV	Yes	Mediastinal Nodes, Bone	No	Yes				Pembrolizum ab
USO-041	68/F	Caucasian	NSCLC	IV	Yes	Mediastinum	Yes	No	Paclitaxel	Carboplatin	Bevacizumab	Nivolumab

Table S2. Patient tumor whole exome sequencing and ATLAS screening results for lung cancer observational study (see excel file Table S2 (lung_seq).xlsx)

Table S3. B16F10 whole exome sequencing and ATLAS screening results (see excel file Table S3 (mATLAS_seq).xlsx)

All non-synonymous mutations are listed by a Genocoea gene ID, chromosome, gene name, transcript variant (amino acid change), and effect. All DNA mutation fragments that could be synthesized (1663) were screened in mouse ATLAS. Normalized CD8 IFN γ and TNF α cytokine secretion are presented. A subset of 174 mutations (roughly equal numbers of stimulatory, non-responder, and inhibitory antigens) were re-screened in two follow-up screens and the average data across all 3 screens was used to rank antigens for IFN γ from most stimulatory (1) to most inhibitory (174) relative to negative controls.

Table S4. Antigens included in vaccine formulations and evaluated in the B16F10 model

Neoantigens and TAA		
Gene	Neoantigen 27merSLP	WT 27merSLP
<i>Gal3St1</i>	AAPCSPIPNEPVAAT A ANGSAGGCQPR	AAPCSPIPNEPVAAT P ANGSAGGCQPR
<i>M27</i>	REGVELCPGNKY E MRRHGTTTHSLVIHD	REGVELCPGNKY T RRHGTTTHSLVIHD
<i>M30</i>	PSKPSFQEFVDW E NVSPELNSTDQPFL	PSKPSFQEFVDW K VSPELNSTDQPFL
<i>Trp2</i>	VYDFFVWL	VYDFFVWL

Inhibigens		
Gene	Neoantigen 27merSLP	WT 27merSLP
<i>Abca17</i>	FYNYPLKSKFQL P YIPSKSETLKAVTE	FYNYPLKSKFQL A YIPSKSETLKAVTE
<i>Taar9</i>	EEGIEELVVALTCVGG W QAPLNQNWVL	EEGIEELVVALTCVGG C QAPLNQNWVL
<i>Asb14</i>	LDRPICPSLGF T SPLNSLDMSKNMSDD	LDRPICPSLGF A SPLNSLDMSKNMSDD
<i>Mmp9 FS</i>	VFFFSGRKCGCTQARPCWAPGVWISWV	VFFFSGRQMWVYTGKTVLGPRSLDKLG

Gal3St1 galatosyl-3-O-sulfoltransferase
Abca17 ATP binding cassette
Taar9 Trace amine associated receptor 9
Asb14 Ankyrin Repeat Domain-Containing SOCS Box Protein
Mmp9 Matrix metalloprotease frameshift mutation

Table S5. Patient tumor whole exome sequencing and ATLAS screening results for GEN-009 personalized cancer vaccine clinical trial (see excel file Table S5 (GEN009_seq).xlsx)

Table S6. Post-vaccination (Day 50) Responses^a by Fluorospot Assay

Patient	Tumor Type	<i>ex vivo</i>				IVS				Any Assay ^b
		PBMC	CD4	CD8	Total Pos	PBMC	CD4	CD8	Total Pos	Total Pos
A	SqNSCLC	60%	10%	40%	80%	100%	67%	33%	100%	100%
B	Urothelial	75%	50%	38%	75%	75%	100%	63%	100%	100%
C	Melanoma	63%	6%	38%	81%	100%	100%	100%	100%	100%
E	Urothelial	31%	100%	69%	100%	69%	85%	31%	85%	100%
F	NSCLC	45%	55%	45%	82%	82%	100%	64%	100%	100%
G	Urothelial	69%	77%	15%	85%	100%	77%	62%	100%	100%
H	Bladder	63%	38%	75%	100%	88%	88%	63%	88%	100%
K	SCHNCC	22%	89%	11%	89%	78%	78%	33%	78%	89%

a. Number of positive peptides/total peptides immunized. Responses were defined as fluorospot SFC that exceeded the limit of detection (LOD), empirically defined for each assay, and for which the P-value between test and negative control wells was ≤ 0.05 by the DFR(eq) test

b. Any analyte, any T cell type

Table S7. Median Responder Rate¹ by Pool

	<i>IFNγ</i>	<i>TNFα</i>	<i>dual</i>
<i>CD4</i>	88%	75%	88%
<i>CD8</i>	63%	13%	50%
<i>PBMC</i>	88%	75%	88%

¹D50 positive statistical immune response and a respective negative statistical immune response at Baseline. If a subject was response positive at both Screening and D50 by the DFR(eq) test ($p \leq 0.05$), the D50 outcome was considered a response if the magnitude of response post-screening was greater as assessed by a Wilcoxon rank sum test ($p \leq 0.05$).

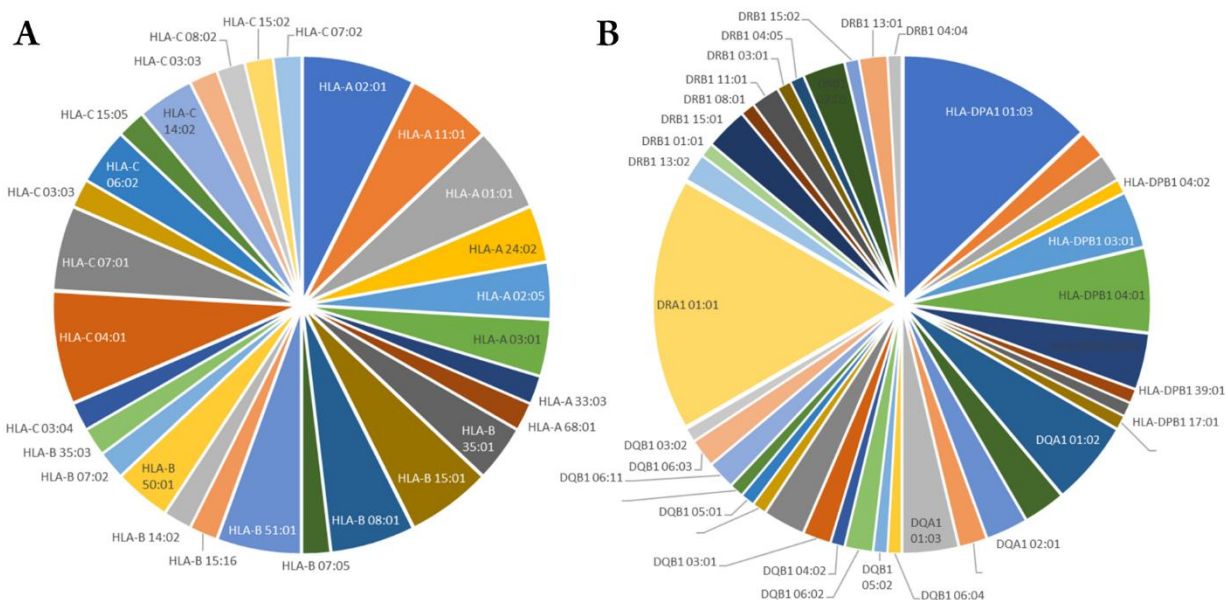


Figure S1. HLA types represented in the ATLAS screens of the lung cohort. A, HLA class I. B, HLA class II. The HLA haplotype of each participant was determined from their tumor exome, normal exome, and/or RNAseq data using OptiType and seq2HLA software. The number of times that each allele is represented in the cohort are depicted.

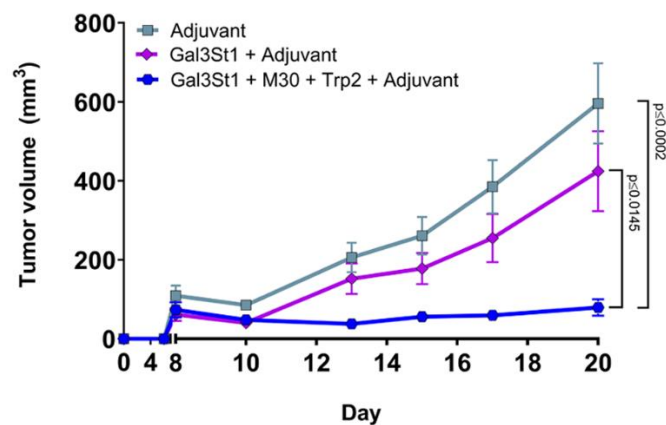


Figure S2: Gal3St1 vaccination alone is insufficient for complete B16F10 melanoma tumor regression. Mean tumor growth kinetics after therapeutic immunization with indicated neoantigen peptide vaccine + adjuvant (CpG, 3DPHAD, QS21) or adjuvant alone on days 3, 10, and 17 ($n \geq 9$ per group; ulcerated tumors censored from analysis). P-values at day 20 determined by one-way ANOVA.

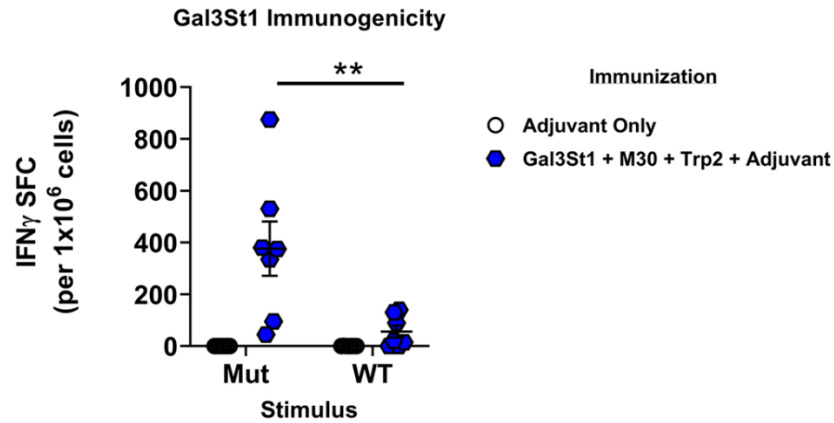


Figure S3: T cell responses to Gal3St1 after vaccination are specific for to the mutation, not the wild type sequence. IFN γ ELISpot analysis was performed on splenocytes from vaccinated, B16F10 tumor-bearing mice using Gal3St1 specific overlapping peptides (OLPs) or wild-type OLP counterparts. Data are a representative set of 2 independent experiments. Statistical analysis was performed using a T-test **p = 0.01.

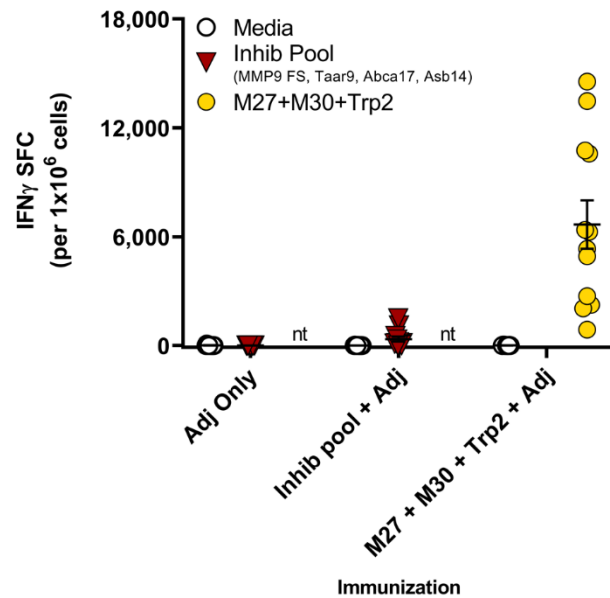


Figure S4: Therapeutic immunization with a vaccine containing Inhibigen SLPs results in fewer IFN γ -secreting T cells compared to the same vaccine in the absence of Inhibigens. IFN γ ELISpot analysis was performed on whole blood PBMCs from vaccinated, B16F10 tumor-bearing mice on Day 16 using OLPs spanning the SLPs included in each vaccine formulation. The adjuvant group was re-stimulated with OLPs spanning the vaccine containing the Inhibigen SLPs. Data are representative of two independent experiments. nt denotes “not tested”.

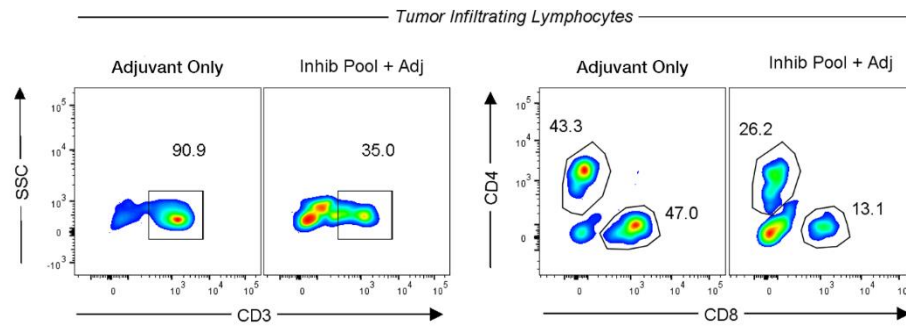


Figure S5: Therapeutic immunization with a vaccine containing Inhibigen SLPs results in reduced T cell infiltration into tumors. Flow cytometry showing the percentage of T cell infiltration into tumors of Inhibigen immunized or control mice. Data represents TIL pools of 4 mice/group harvested on Day 18 post-tumor implantation. Quantification is defined by the proportion of B-cell and NK cell depleted, CD45⁺ lymphocytes. Right bar graph shows T cells as a proportion of total live cells.

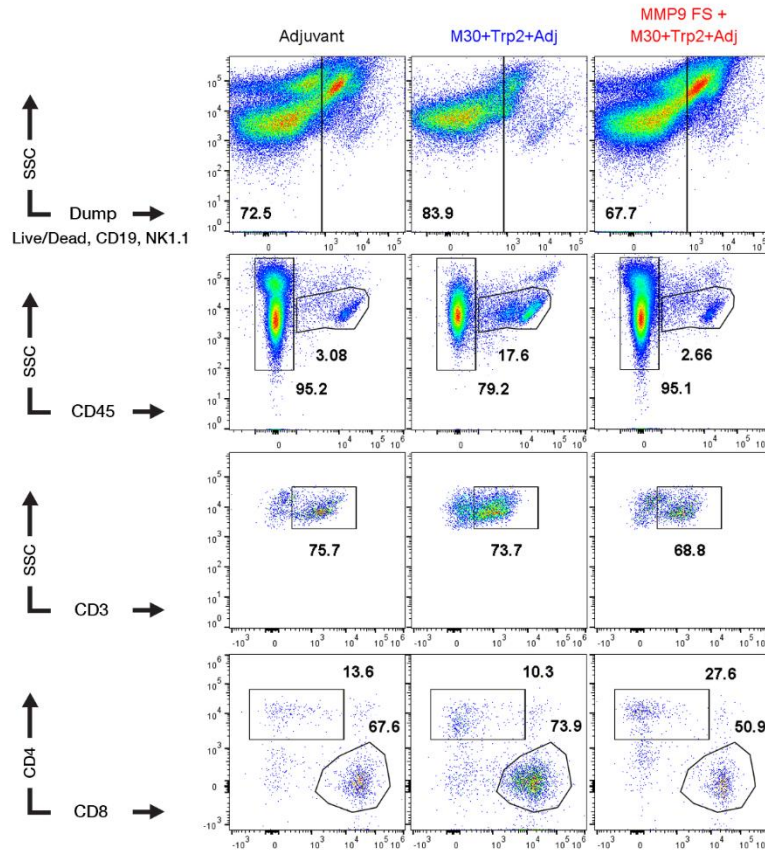


Figure S6: Coformulation of the MMP9_{FS} Inhibigen with a protective therapeutic vaccine results in reduced CD8⁺ T cell infiltration into tumors. Flow cytometry plots gating on live, CD19^{neg}, NK1.1^{neg} cells showing reduced CD45⁺ cells within tumors from mice vaccinated therapeutically with a vaccine containing the MMP9_{FS} inhibigen or the same vaccine in the absence of MMP9_{FS}. Mice receiving the protective vaccine (M30+Trp2) had significantly expanded populations of CD45⁺ lymphocytes, predominantly T cells (middle), and enriched for the CD8⁺ T cell subsets in their tumors. Tumors from mice receiving the MMP9_{FS}-containing vaccine had similar TIL composition to the mice receiving adjuvant alone. Data shown are gated on the CD45⁺ cells within the total population of tumor digest, and subsequent CD3⁺, CD4⁺/CD8⁺ are gated on the previous parent gate. Each is the pool of 4 tumors per group.

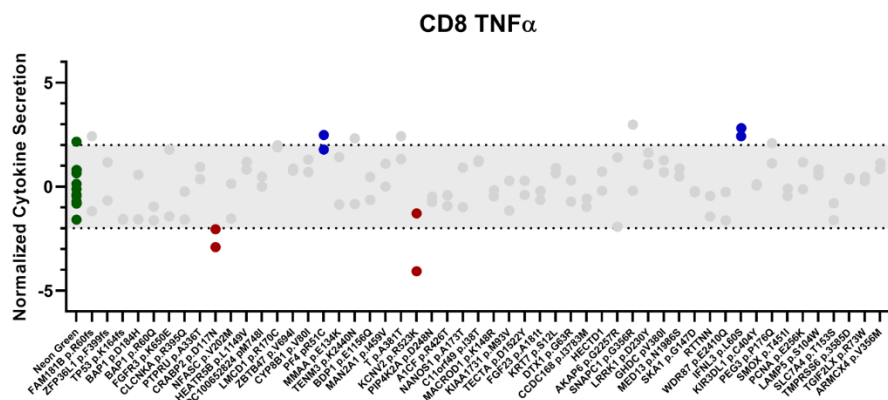
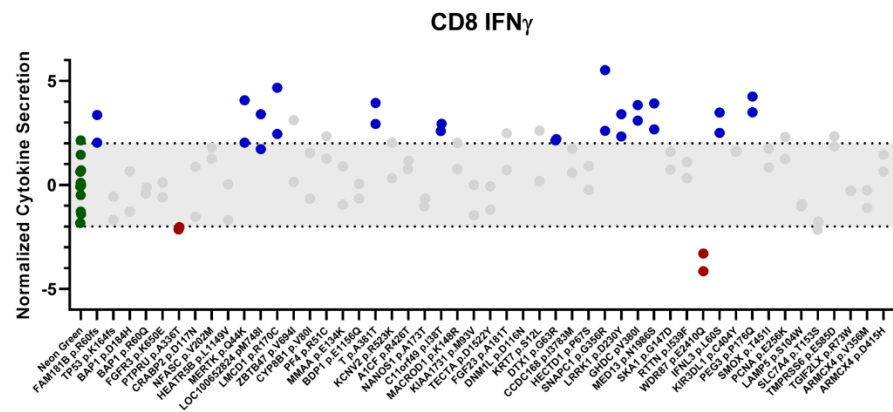
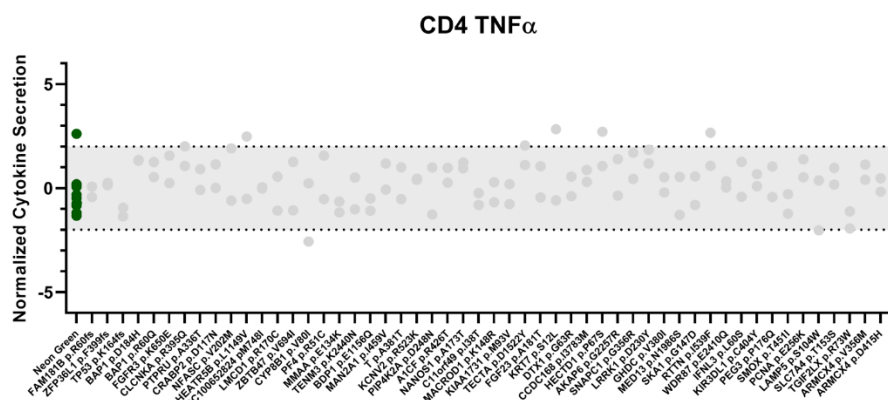
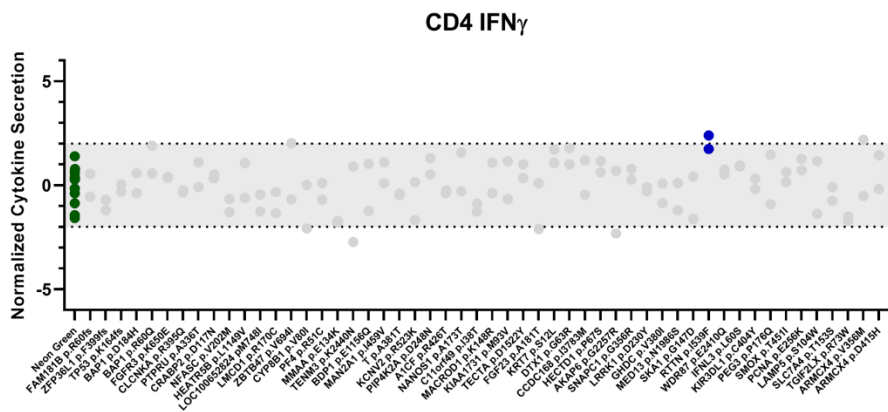
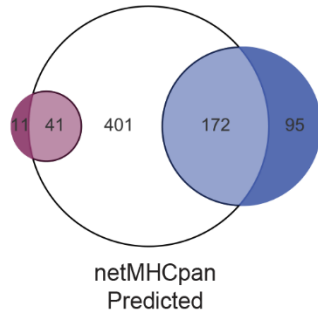


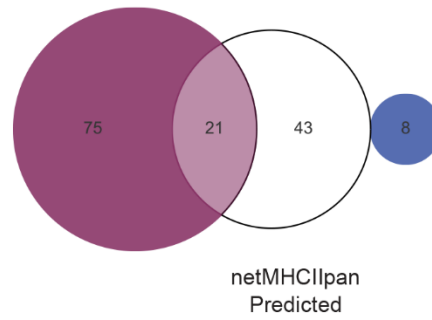
Figure S7. Representative ATLAS plot. Representative ATLAS screening results are shown for patient B. MDDCs derived from the patient's blood were pulsed with *E. coli* individually expressing each mutation identified in their tumor then sorted CD4⁺ or CD8⁺ T cells were added and incubated overnight. The next day, cytokines present in the supernatants were measured by MSD assay. Green symbols represent baseline controls, blue symbols represent neoantigens, burgundy symbols represent Inhibigens for each T cell type and cytokine evaluated. Neoantigens represented in blue were prioritized for inclusion in their vaccine formulation.

A

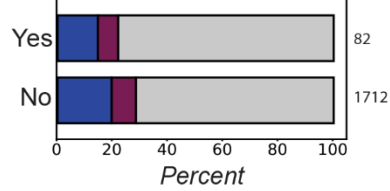
MHC class I epitope predictions

**B**

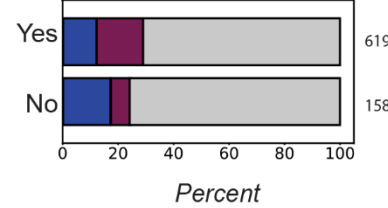
MHC class II epitope predictions

**C**

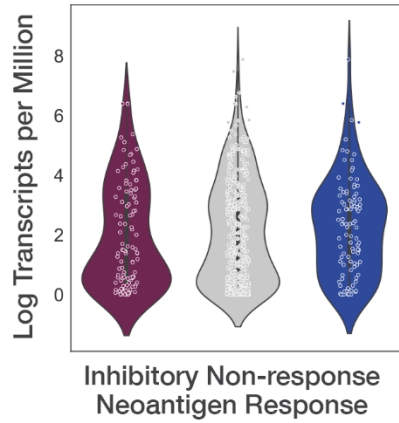
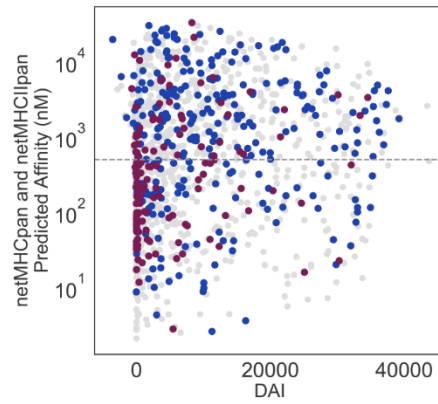
Mutation in Cancer Gene

**D**

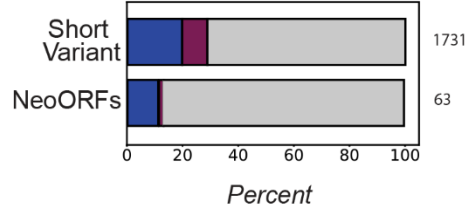
Variant Detected in RNA

**E**

Gene Expression Levels

**F****G**

Mutation Type

**H**

Comparison of Algorithm and ATLAS

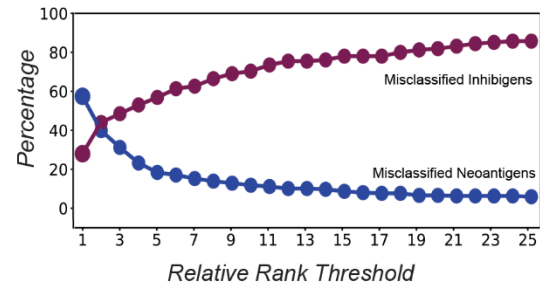


Figure S8. Neoantigen characteristics in the clinical trial cohort of patients

A, and B, Venn Diagrams comparing ATLAS-identified T cell responses with NetMHCpan 4.0 predictions with a peptide length of 9aa and NetMHCIpan 4.0 predictions using a peptide length of 15aa; in both cases the cutoff was a rank threshold of 2%. Blue circles represent neoantigens, burgundy circles represent Inhibigens, and open circles were predicted but not confirmed epitopes. C-G, Classification of ATLAS results according to commonly used *in silico* prediction down-selection criteria. Relative proportion of neoantigens (blue), Inhibigens (burgundy), and non-antigenic (grey) mutations are indicated. C, Antigens classified by if they are a known cancer gene, x-axis is the proportion of mutations. D, Classification of responses by if the mutation was expressed by RNAseq analysis. E, Violin plots showing expression levels of transcripts corresponding to mutations screened, represented as transcripts per million (TPM). F, Minimum predicted affinity (nM) plotted against the maximum calculated differential agretopicity index (DAI) for each SNV. DAI is calculated as the difference between MHC binding affinities of wild type and mutant peptides. G, Effect of mutation type on neoantigen / Inhibigen outcome. Short variant includes substitutions at one or more nucleotides. Frameshift and stop-loss mutations are counted as NeoORFs. H, Tuning rank threshold parameters for NetMHCpan / NetMHCIpan algorithm to match antigen classification by ATLAS. The red line represents the percent of Inhibigens identified by ATLAS that are classified as binding by the algorithms. The blue line represents the percent of ATLAS-identified neoantigens that are classified as non-binding by algorithms.

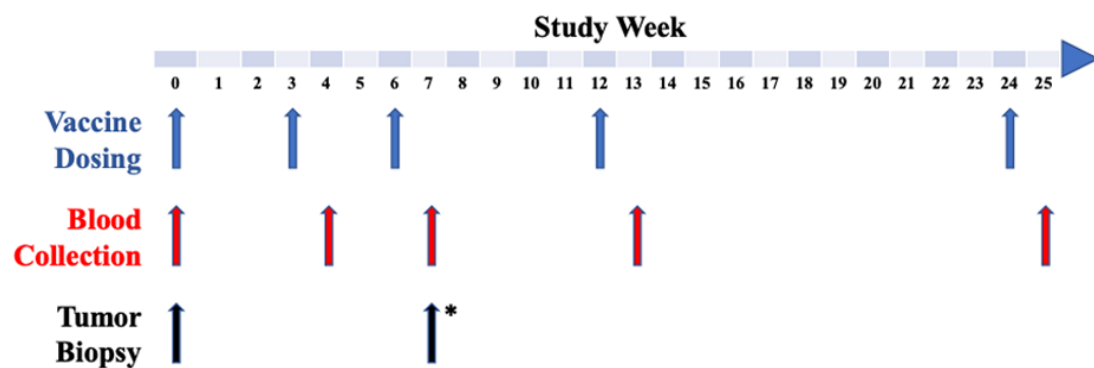


Fig S9. GEN-009 Vaccination and Immunogenicity Assessment Schedule. The schedule of vaccine dosing (blue), blood collection (red) and tumor biopsy (black) are indicated by week of the study. Asterisk indicates an optional collection.